Fast Multipole Formulation for PEEC Frequency Domain Modeling

Giulio Antonini

Dept. of Electrical Engineering,
University of L'Aquila
67040, Poggio di Roio, AQ, ITALY
antonini@ing.univaq.it

Keywords: Integral equations, Partial Element Equivalent Circuit Method, Fast Multipole Method.

Abstract

This paper presents a tutorial and overview of the Fast Multipole Method (FMM) which is used to improve the performances of the Partial Element Equivalent Circuit (PEEC) technique in the frequency domain. Aim of the tutorial is to introduce the reader with the basic theory of the Fast Multipole Method. Step-by-step implementations of FMM are detailed providing useful guidelines for the potential user. The FMM is used in the PEEC framework showing how to compute PEEC parameters in a more efficient way without compromising the accuracy. Several examples are presented in which FMM has proven to be useful. A comprehensive list of references is also provided to allow the interested readers to go deeper inside FMM.

1 Introduction

Realistic Electromagnetic Compatibility (EMC) and Electrical Interconnect and Package (EIP) problems require flexible computational tools which can provide meaningful solutions for many different problems such as lightning, high frequency on-chip interconnects and Printed Circuit Board (PCB) modeling. Over the last few years the continuous increase of speed of digital electronic chips and increased frequencies of RF circuits has made their electromagnetic modeling an extremely challenging task. Clock rates of several hundred megahertz and signal rise/fall times of less than 100 ps cause the spectra of waveforms to extend up to 10 GHz. At these frequencies inductive and capacitive coupling between different conductors is no longer negligible and an accurate electromagnetic modeling is required to provide good simulations. In order to incorporate all the effects suitable models are required. On the other hand the intrinsic three-dimensional (3-D) nature of realistic problems limits the use of Transverse Electromagnetic waves (TEM) or quasi-TEM mode lumped circuit models. Among all the numerical methods of particular interest to high frequency high-speed mixed-signal circuit electrical analysis is the Partial-Element Equivalent Circuit (PEEC) method [1-3]. The PEEC formulation results in a circuit model which includes all the retardation effects. Moreover it is compatible with a non-linear circuit simulation framework like SPICE. These two features make the PEEC method especially tailored for studying mixed electromagnetic-circuit problems such as high-

speed electrical interconnect and package as well as for other EMC problems, such as power/ground-plane EMI de-coupling [4] and PCBs analysis.
This paper deals with the incorporation of the Fast Multipole Method (FMM) into the PEEC method in the frequency domain. In the last decade FMM has been widely used in conjunction with the Method of Moments (MoM) in the frequency domain for the analysis of scattering problems of electrically large objects [5,6]. More recently the FMM time domain counterpart has been developed by Michiellsen's group [7-9] and adopted to study scattering from closed surfaces [10] and to analyze EMC/EMI problems [11]. As FMM is specially suitable for efficient computation of the dense matrix-vector product as those arising from integral methods it can be successfully used to enhance also the PEEC method. In particular in this tutorial paper FMM-based expressions of mutual partial inductances and potential coefficients are presented and it is shown how the proposed approach can speed-up their evaluation. As a consequence the matrix-vector products arising from the Modified Nodal Analysis (MNA) [12] are computed more efficiently.
The paper is organized as follows: Section 2 is devoted to a short overview of the PEEC method, then FMM theory is described in Section 3. The evaluation of PEEC parameters, partial inductances and potential coefficients, by using the FMM method is presented in Section 4; the FMM-based matrix-vector product scheme is assessed in Section 5; Section 6 describes several numerical results. Conclusions are summarized in Section 7.

2 PEEC theory

In the following it is assumed that the space is filled with an uniform dielectric although PEEC models have been developed also for finite dielectrics [3]. PEEC method is derived from the following equation to be enforced in the conductors and dielectrics

$$\hat{n} \times \left(- \vec{\mathbf{E}}_{\mathbf{0}}(\vec{\mathbf{r}}, \omega) + \frac{\vec{\mathbf{J}}(\vec{\mathbf{r}}, \omega)}{\sigma} + j\, \omega \vec{\mathbf{A}}(\vec{\mathbf{r}}, \omega) + \nabla \Phi(\vec{\mathbf{r}}, \omega) \right) = 0 \tag{1}$$

where $\vec{\mathbf{E}}_{\mathbf{0}}$ denotes the external electric field, $\vec{\mathbf{J}}$ is the current density in the conductor, $\vec{\mathbf{A}}$ and Φ are the magnetic vector and electric scalar potentials respectively. The magnetic vector potential $\vec{\mathbf{A}}$ and the electric scalar potential Φ at any point $\vec{\mathbf{r}} = (\mathbf{x}, \mathbf{y}, \mathbf{z})$ are given by

$$\vec{\mathbf{A}}(\vec{\mathbf{r}}, \omega) = \frac{\mu}{4\pi} \int_{V'} G(\vec{\mathbf{r}}, \vec{\mathbf{r}}') \vec{\mathbf{J}}(\vec{\mathbf{r}}', \omega)\, dV' \qquad \Phi(\vec{\mathbf{r}}, \omega) = \frac{1}{4\pi\varepsilon} \int_{S'} G(\vec{\mathbf{r}}, \vec{\mathbf{r}}') \rho(\vec{\mathbf{r}}', \omega)\, dS' \tag{2}$$

where ρ the surface charge density and *G* the Green's function for an homogeneous medium

$$G(\vec{\mathbf{r}}, \vec{\mathbf{r}}') = \frac{e^{jk|\vec{\mathbf{r}} - \vec{\mathbf{r}}'|}}{|\vec{\mathbf{r}} - \vec{\mathbf{r}}'|} \tag{3}$$

Substituting the vector and scalar potentials into (1) yields the following integral equation

$$\hat{n} \times \left(-\vec{\mathbf{E}}_{\mathbf{0}}(\vec{\mathbf{r}},\omega) + \frac{\vec{\mathbf{J}}(\vec{\mathbf{r}},\omega)}{\sigma} + j\,\omega\,\mu \int_V G(\vec{\mathbf{r}},\vec{\mathbf{r}}')\vec{\mathbf{J}}(\vec{\mathbf{r}}',\omega)\,dV' + \frac{\nabla}{\varepsilon} \int_{S'} G(\vec{\mathbf{r}},\vec{\mathbf{r}}')\rho(\vec{\mathbf{r}}',\omega)\,dS' \right) = 0 \qquad (4)$$

In order to solve integral equation (4) current and charge densities are discretized into volume and surface cells respectively. Applying Galerkin method allows obtaining PEEC models with conventional circuit elements. Ohmic losses are taken into account by longitudinal resistances, the magnetic field coupling is represented by means of partial inductances and the last term in equation (4) corresponds to the voltage drop expressed in terms of potential coefficients. Enforcing Kichhoff's current law (KCL) to each node and Kirchhoff's voltage law (KVL) to each loop of the equivalent circuit leads to the standard MNA formulation [12].

$$\begin{bmatrix} -A & -R - j\omega L_p \\ j\omega P^{-1} + Y_{lumped} & -A^T \end{bmatrix} \begin{bmatrix} V \\ I_L \end{bmatrix} = \begin{bmatrix} V_s \\ I_s \end{bmatrix} \qquad (5)$$

where A is the connectivity matrix, P is the potential coefficients matrix taking into account the electric field coupling, L_p is the partial inductances matrix which reproduces the magnetic field coupling, Y_{lumped} represents the admittance matrix of lumped elements, V_s and I_s are lumped voltage and current sources respectively, V and I_L are potentials to infinity and longitudinal currents. If charges Q are assumed as unknowns instead of potentials to infinity V the following alternative formulation is easily found

$$\begin{bmatrix} -AP & -R - j\omega L_p \\ j\omega \coprod + Y_{lumped} P & -A^T \end{bmatrix} \begin{bmatrix} Q \\ I_L \end{bmatrix} = \begin{bmatrix} V_s \\ I_s \end{bmatrix} \qquad (6)$$

The discretization of integral equation (4) thus gives rise to dense operator matrix. The solution of matrix equation (6) by iterative methods involves many matrix-vector products. This fact can make the solution extremely slow to be obtained when a large number of unknowns is considered and, hence, adopting a technique which enables to significantly accelerate the matrix fill-in process and the computation of matrix-vector products is highly desirable.

3 The Fast Multipole Method

The Fast Multipole Method was introduced by Rokhlin for acoustic wave scattering in two dimensions [13], Lu and Chew [5] applied the FMM method in electromagnetics to compute the scattered field of two-dimensional dielectric coated conducting cylinders and Coifman, Rokhlin and Wandzura [14] extended it to the three-dimensional wave equation. In 1995 Song and Chew [6] introduced a multilevel-FMM based algorithm. More recently Michielssen, Ergin and Shanker proposed its direct time-domain counterpart known as Plane-Wave Time Domain algorithm (PWTD) [7-11]. FMM has been mainly applied to scattering problems that are usually solved writing the corresponding integral equation assuming the induced current distribution as unknown. The Method of Moments (MoM) is used to convert the integral equation to a matrix equation. Scattering computation from large objects is a hard task because of the huge number of unknowns. Solving the matrix equation by means of LU decomposition requires $O(N^3)$ operations. In this case iterative solvers such as the Conjugate Gradient

(CG) allow reducing computational complexity to $O(N^2)$ operations per iteration, since the most costly step is the matrix vector multiplication which becomes the bottleneck. FMM has been found to be effective in speeding-up this process. In the present paper FMM is used to accelerate the computation of PEEC parameters, namely partial inductances L_p and potential coefficients P and, as a consequence, the matrix-vector products which involve these matrices such as L_pI_L and PQ in Equation (6) can be performed in a more efficient way.
The evaluation of these matrix-vector products allows obtaining the effect at each location of basis functions of currents I_L or charges Q due to all the currents I_L or charges Q themselves. A matrix-vector product involving a dense matrix and a dense vector requires N^2 operations, as illustrated in Fig. 1.

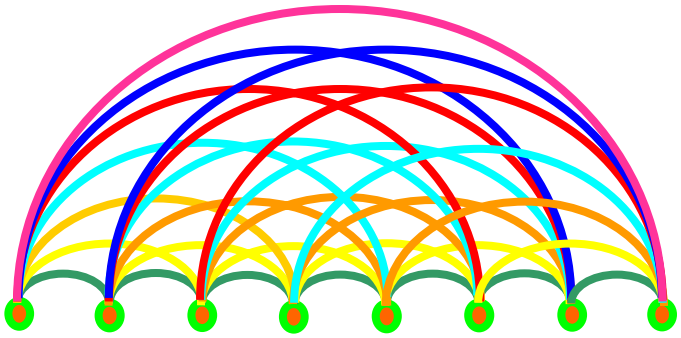

Fig. 1 - One level interaction: all sources "talk" directly to each other.
The number of links is proportional to N^2 where N is the number of sources.

Every source communicates with each other source directly. If the sources are grouped together into G groups, the number of the interactions can be significantly reduced. Fig. 2 shows the resulting two-level structure of the interaction among the sources. This type of approach is based on certain decomposition of the kernel of the original integral problem. The decomposition reduces the connections among basis functions belonging to different groups and this is the reason of the speed-up that the FMM techniques provide in computing matrix-vector products.

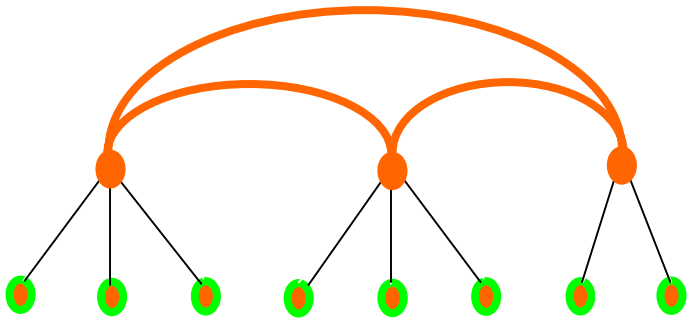

Fig. 2 - Two level interaction: sources "talk" indirectly to each other.
The number of links is proportional to G^2 where G is the number of groups of sources.

The Fast Multipole Method (FMM) is based on two elementary identities which can be found in many texts and handbooks on mathematical methods such as [15] and [16]. Let's consider a target

(observation) point $\vec{\mathbf{r}}_m$ and a source point $\vec{\mathbf{r}}_n$. The first expansion represents the Green's function by using the Gegenbauer's addition theorem:

$$\frac{e^{jk_0|\vec{\mathbf{r}}_m-\vec{\mathbf{r}}_n|}}{|\vec{\mathbf{r}}_m-\vec{\mathbf{r}}_n|}=\frac{e^{jk_0|\vec{\mathbf{R}}+\vec{\mathbf{d}}|}}{|\vec{\mathbf{R}}+\vec{\mathbf{d}}|}=j\,k_0\sum_{l=0}^{\infty}(-1)^l(2l+1)j_l(k_0d)h_l^{(1)}(k_0R)P_l\left(\hat{\mathbf{d}}\cdot\hat{\mathbf{R}}\right),\quad R>d \tag{7}$$

where j_l is a spherical Bessel function of the first kind, $h_l^{(1)}$ is a spherical Hankel function of the first kind and P_l is a Legendre polynomial and $R>d$. The second expansion allows to expand the product $j_l(k_0d)P_l\left(\hat{\mathbf{d}}\cdot\hat{\mathbf{R}}\right)$ in propagating plane waves as follows:

$$j_l(k_0d)P_l\left(\hat{\mathbf{d}}\cdot\hat{\mathbf{R}}\right)=\frac{1}{4\pi j^l}\int_{S^2}e^{j\vec{\mathbf{k}}_0\cdot\vec{\mathbf{d}}}P_l\left(\hat{\mathbf{k}}_0\cdot\hat{\mathbf{R}}\right)d^2\hat{\mathbf{k}}_0 \tag{8}$$

where $\vec{\mathbf{k}}_0=k_0\hat{\mathbf{k}}_0$ and the notation $\int_{S^2}\bullet\,d^2\hat{\mathbf{k}}_0$ stands for integration over the unit sphere:

$$\int_{S^2}\bullet\,d^2\hat{\mathbf{k}}_0=\int_0^{2\pi}\int_0^{\pi}\bullet\sin\theta d\theta d\phi\ \text{ and }\ \hat{\mathbf{k}}_0=\sin\theta\cos\phi\,\hat{x}+\sin\theta\sin\phi\,\hat{y}+\cos\theta\,\hat{z} \tag{9}$$

Combining Equations (7) and (8) we obtain:

$$\frac{e^{jk_0|\vec{\mathbf{r}}_m-\vec{\mathbf{r}}_n|}}{|\vec{\mathbf{r}}_m-\vec{\mathbf{r}}_n|}=\frac{j\,k_0}{4\pi}\int_{k_0}e^{j\vec{\mathbf{k}}_0\bullet\vec{\mathbf{d}}}\left[\sum_{l=0}^{\infty}j^l(2l+1)h_l^{(1)}(k_0R)P_l\left(\hat{\mathbf{k}}_0\bullet\hat{\mathbf{R}}\right)\right]d^2\hat{\mathbf{k}}_0\qquad R>d \tag{10}$$

In accordance with the FMM the *N* unknowns of the problem (currents or charges), introduced for the discretization of equation (4) are subdivided into *G* groups, with each group assigned *M=N/G* unknowns. Let's assume that the target (observation) point $\vec{\mathbf{r}}_m$ belongs to a group with a center $\vec{\mathbf{r}}_a$ and the source point $\vec{\mathbf{r}}_n$ belongs to a group with center $\vec{\mathbf{r}}_b$. Thus we may write

$$\vec{\mathbf{r}}_m-\vec{\mathbf{r}}_n=\vec{\mathbf{R}}+\vec{\mathbf{d}}=\left(\vec{\mathbf{r}}_m-\vec{\mathbf{r}}_a\right)+\left(\vec{\mathbf{r}}_a-\vec{\mathbf{r}}_b\right)+\left(\vec{\mathbf{r}}_b-\vec{\mathbf{r}}_n\right)=\vec{\mathbf{r}}_{ma}+\vec{\mathbf{r}}_{ab}-\vec{\mathbf{r}}_{nb} \tag{11}$$

where $\vec{\mathbf{r}}_a-\vec{\mathbf{r}}_b\equiv\vec{\mathbf{r}}_{\mathbf{ab}}=\vec{\mathbf{R}}$ and $\left(\vec{\mathbf{r}}_m-\vec{\mathbf{r}}_a\right)-\left(\vec{\mathbf{r}}_n-\vec{\mathbf{r}}_b\right)=\vec{\mathbf{r}}_{ma}-\vec{\mathbf{r}}_{nb}\equiv\vec{\mathbf{d}}$. The approximation of the Green's function (3) is established from an elementwise approximation. To obtain an elementwise expansion we use the source center $\vec{\mathbf{r}}_b$ and the target center $\vec{\mathbf{r}}_a$ as the reference points and expand the Green's function about $\vec{\mathbf{r}}_a-\vec{\mathbf{r}}_b$, see Fig. 3.

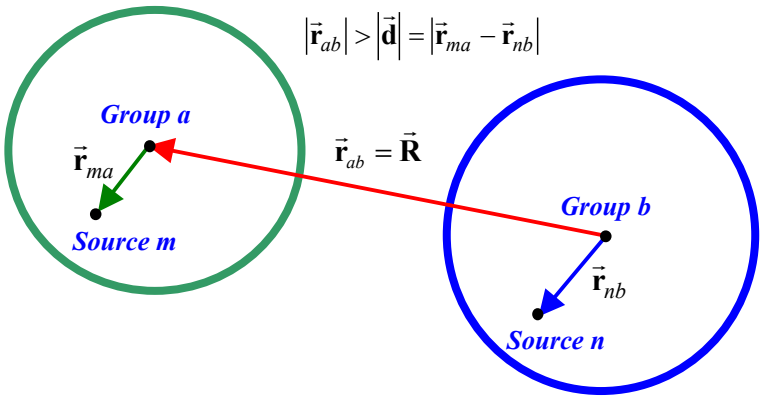

Fig. 3 – Expansion about $\vec{\mathbf{r}}_a - \vec{\mathbf{r}}_b$ and separation of $\vec{\mathbf{r}}_{ma}$ and $\vec{\mathbf{r}}_{nb}$.

Truncating the infinite sum in (7) by retaining only $L+1$ terms leads to the following approximation of the scalar Green's function

$$\begin{aligned}\frac{e^{jk_0|\vec{\mathbf{r}}_m-\vec{\mathbf{r}}_n|}}{|\vec{\mathbf{r}}_m-\vec{\mathbf{r}}_n|} &\cong \frac{j\,k_0}{4\pi}\int_{k_0} e^{j\vec{\mathbf{k}}_0\bullet(\vec{\mathbf{r}}_{ma}-\vec{\mathbf{r}}_{nb})}\left[\sum_{l=0}^{L} j^l(2l+1)h_l^{(1)}(k_0R)P_l\left(\hat{\mathbf{k}}_0\bullet\hat{\mathbf{R}}\right)\right]d^2\hat{\mathbf{k}}_0 \\ &= \frac{j\,k_0}{4\pi}\int_{S^2} e^{j\vec{\mathbf{k}}_0\bullet(\vec{\mathbf{r}}_{ma}-\vec{\mathbf{r}}_{nb})}\alpha_{ab}^{L}\left(\hat{\mathbf{R}}\bullet\hat{\mathbf{k}}_0\right)d^2\hat{\mathbf{k}}_0\end{aligned} \tag{12}$$

where

$$\alpha_{ab}^{L}\left(\hat{\mathbf{R}}\bullet\hat{\mathbf{k}}_0\right)=\sum_{l=0}^{L} j^l(2l+1)h_l^{(1)}(k_0R)P_l\left(\hat{\mathbf{k}}_0\bullet\hat{\mathbf{R}}\right),\quad a,b=1,\ldots G \tag{13}$$

The number of the $L+1$ terms to be retained depends on the desired accuracy. The integration in Equation (12) is done numerically. There several possibilities for the choice of sample points on the unit sphere S^2. The most straightforward is the uniform distribution of points:

$$\phi_i = \frac{2\pi}{I}i \qquad \theta_j = \frac{\pi}{J}j \tag{14}$$

being I and J the number of sampling points of $\phi \in [0-2\pi]$ and $\theta \in [0-\pi]$.
This choice has the clear advantage of being simple but doesn't allow a very accurate integration of spherical harmonics. It requires twice more points than the Gauss-Legendre points. The optimal choice of sample points are uniform points for ϕ and Gauss-Legendre points for θ. With this choice of points it is possible to integrate exactly all the spherical harmonics of order L using $L+1$ points in the θ direction and $2L+2$ points in the ϕ direction.

The function $\alpha_{ab}^{L}\left(\hat{\mathbf{R}}\bullet\hat{\mathbf{k}}_{\mathbf{0}}\right)$ is defined for each different groups pair and it depends on the unit vector $\hat{\mathbf{k}}_{\mathbf{0}}$. Fig. 4 shows the behavior of function $\alpha_{ab}^{L}\left(\hat{\mathbf{R}}\bullet\hat{\mathbf{k}}_{\mathbf{0}}\right)$ for L=14, $k_0 R$=30 and different values of the angle between $\hat{\mathbf{R}}$ and $\hat{\mathbf{k}}_{\mathbf{0}}$, being $\cos\theta = \hat{\mathbf{R}}\bullet\hat{\mathbf{k}}_{\mathbf{0}}$.

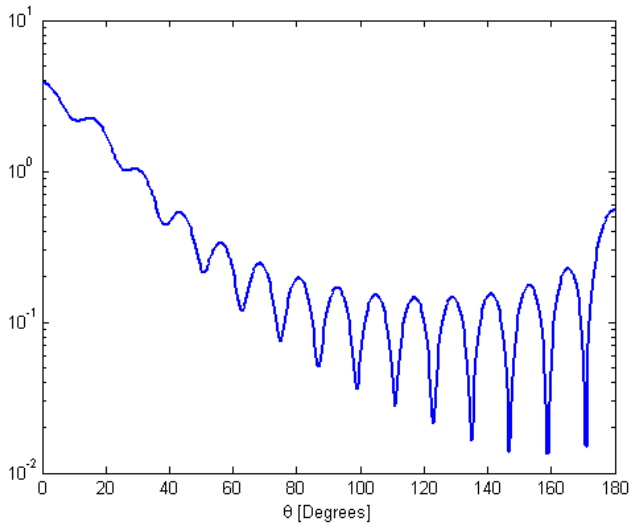

Fig. 4 – Amplitude of $\alpha_{ab}^{L}\left(\hat{\mathbf{R}}\bullet\hat{\mathbf{k}}_{\mathbf{0}}\right)$ in Equation (13) as function of θ for L=14 and $k_0 R$=30 where $\cos\theta = \hat{\mathbf{R}}\bullet\hat{\mathbf{k}}_{\mathbf{0}}$.

4 PEEC parameters computation

The above outlined approach to represent the Green's function can be used to obtain approximated coefficients describing the electromagnetic coupling. According to the PEEC method the magnetic and electric field couplings are described by partial inductances L_P and potential coefficients P matrices which must be evaluated to fill in the MNA matrix (5) or (6). FMM allows representing these matrices separating the contribution due to basis functions (currents and charges) belonging to groups satisfying the condition $R > d$ (non-near neighbors) from that of groups which don't accomplish it (near neighbors). Furthermore the first contribution is factorized in such a way to de-couple the sources. If A is the generic matrix describing the coupling, by using the FMM expansion it can be expressed as

$$A = A^{near} + A^{far} \tag{15}$$

and A^{far} matrix entries can be factored as $A_{mn}^{far} = \overline{V}_{ma}^{t}\widetilde{\alpha}_{ab}\overline{V}_{nb}$, where indexes a and b refer to groups to which sources m and n belong. A plane-wave basis has proven to diagonalize the matrix $\widetilde{\alpha}_{ab}$. This result was originally achieved by Rokhlin [13]. As a consequence of that the non-near neighbors contribution is factorized into a product of a vector, a diagonal matrix and a vector. It is worth to note that vectors $\overline{V}_{ma}^{t}$ and $\overline{V}_{nb}$ can be re-used in computing all the interactions involving sources m and n respectively and need to be computed just once at the beginning. Furthermore it also possible to pre-compute the function $\widetilde{\alpha}_{ab}$, as it will be clarified in the following Sections.

4.1 Partial inductances computation

The standard expression for volume mutual partial inductances between two different inductive cells *m* and *n* is given by

$$L_{p,mn} = \frac{\mu \cos\theta_{mn}}{4\pi\, S_m S_n} \int_{V_m} \int_{V_n} G(\vec{\mathbf{r}}_m, \vec{\mathbf{r}}_n)\, dV_m\, dV_n \tag{16}$$

where $\cos\theta_{mn}$ takes into account the direction of current basis functions *m* and *n*.
Let's assume that inductive cells *m* and *n* belong to groups *a* and *b* which satisfy the condition $R > d$ required by the spectral representation (10) to be valid. Under this hypothesis, taking into account the approximated form of the free space Green's function $G(\vec{\mathbf{r}}_m, \vec{\mathbf{r}}_n)$ given by Equation (12) we can rewrite the partial inductance $L_{p,mn}$ as:

$$L_{p,mn} = \frac{jk_0 \mu \cos\theta_{mn}}{(4\pi)^2 S_m S_n} \int_{k_0} \left[\int_{V_m} e^{j\vec{\mathbf{k}}_0 \bullet \vec{\mathbf{r}}_{ma}}\, dV_m \right] \alpha_{ab}^{L}\left(\hat{\mathbf{r}}_{ab} \bullet \hat{\mathbf{k}}_0\right) \left[\int_{V_n} e^{-j\vec{\mathbf{k}}_0 \bullet \vec{\mathbf{r}}_{nb}}\, dV_n \right] d^2\hat{\mathbf{k}}_0 \tag{17}$$

This expression can be rewritten in a more compact form in terms of volume field and source functions $F_m^v(\hat{\mathbf{k}}_0)$ and $S_n^v(\hat{\mathbf{k}}_0)$ respectively which are scalar functions of $\hat{\mathbf{k}}_0$ defined for every cells pair *m* and *n*.

$$F_m^v(\hat{\mathbf{k}}_0) = \int_{V_m} e^{j\vec{\mathbf{k}}_0 \bullet \vec{\mathbf{r}}_{ma}}\, dV_m \quad , \qquad m = 1, \ldots, N \tag{18a}$$

$$S_n^v(\hat{\mathbf{k}}_0) = \int_{V_n} e^{-j\vec{\mathbf{k}}_0 \bullet \vec{\mathbf{r}}_{nb}}\, dV_n = F_m^{v\,*}(\hat{\mathbf{k}}_0) \qquad n = 1, \ldots, N \tag{18b}$$

where $\vec{\mathbf{r}}_{ma}$ and $\vec{\mathbf{r}}_{nb}$ are the relative vectors of cells *m* and *n* with respect to the centers of groups *a* and *b* to which they belong. Substituting Equations (18a,b) into Equation (17) yields

$$\begin{aligned} L_{p,mn} &= \frac{jk_0 \mu \cos\theta_{mn}}{(4\pi)^2 S_m S_n} \int_{k_0} F_m^v(\hat{\mathbf{k}}_0)\, \alpha_{ab}^{L}\left(\hat{\mathbf{r}}_{ab} \bullet \hat{\mathbf{k}}_0\right) S_n^v(\hat{\mathbf{k}}_0)\, d^2\hat{\mathbf{k}}_0 \\ &= \frac{jk_0 \mu \cos\theta_{mn}}{(4\pi)^2 S_m S_n} \int_{k_0} F_m^v(\hat{\mathbf{k}}_0)\, \alpha_{ab}^{L}\left(\hat{\mathbf{r}}_{ab} \bullet \hat{\mathbf{k}}_0\right) F_m^{v\,*}(\hat{\mathbf{k}}_0)\, d^2\hat{\mathbf{k}}_0 \end{aligned} \tag{19}$$

which represents the FMM approximation of the partial inductance $L_{p,mn}$.

4.2 Potential coefficients computation

Similarly the PEEC method models electric field coupling between conductive regions *m* and *n* by means of potential coefficient P_{mn} given by a double folded surface integral as

$$P_{mn} = \frac{1}{4\pi\,\varepsilon\,A_m A_n} \int_{A_m} \int_{A_n} G(\vec{\mathbf{r}}_m, \vec{\mathbf{r}}_n)\, dA_m\, dA_n \tag{20}$$

where A_m and A_n represent surface areas of patches *m* and *n*. Under the same hypothesis ensuring the validity of Gegenbauer's addition theorem, a multipole representation of potential coefficient P_{mn} can be obtained. Using the Green's function approximation given by Equation (12), truncating the infinite sum in (12) to the first *L+1* terms leads to the following form of potential coefficient P_{mn}:

$$P_{mn} = \frac{jk_0}{(4\pi)^2\,\varepsilon\,A_m A_n} \int_{k_0} \left[\int_{A_m} e^{j\hat{\mathbf{k}}_0 \bullet \vec{\mathbf{r}}_{mn}}\, dA_m \right] \alpha_{ab}^{L}\left(\hat{\mathbf{r}}_{ab} \bullet \hat{\mathbf{k}}_0\right) \left[\int_{A_n} e^{-j\hat{\mathbf{k}}_0 \bullet \vec{\mathbf{r}}_{nb}}\, dA_n \right] d^2\hat{\mathbf{k}}_0 \tag{21}$$

Two auxiliary functions can be defined as

$$F_m^S\left(\hat{\mathbf{k}}_0\right) = \int_{S_m} e^{j\vec{\mathbf{k}}_0 \bullet \vec{\mathbf{r}}_{ma}}\, dA_m \quad , \qquad m = 1, \ldots, N \tag{22a}$$

$$S_n^S\left(\hat{\mathbf{k}}_0\right) = \int_{S_n} e^{-j\vec{\mathbf{k}}_0 \bullet \vec{\mathbf{r}}_{nb}}\, dA_n = F_n^{S^*}\left(\hat{\mathbf{k}}_0\right) \qquad n = 1, \ldots, N \tag{22b}$$

Equation (21) can be rewritten in a more compact form as

$$\begin{aligned} P_{mn} &= \frac{jk_0}{(4\pi)^2\,\varepsilon\,A_m A_n} \int_{k_0} F_m^S\left(\hat{\mathbf{k}}_0\right) \alpha_{ab}^{L}\left(\hat{\mathbf{r}}_{ab} \bullet \hat{\mathbf{k}}_0\right) S_n^S\left(\hat{\mathbf{k}}_0\right) d^2\hat{\mathbf{k}}_0 = \\ &= \frac{jk_0}{(4\pi)^2\,\varepsilon\,A_m A_n} \int_{k_0} F_m^S\left(\hat{\mathbf{k}}_0\right) \alpha_{ab}^{L}\left(\hat{\mathbf{r}}_{ab} \bullet \hat{\mathbf{k}}_0\right) F_n^{S^*}\left(\hat{\mathbf{k}}_0\right) d^2\hat{\mathbf{k}}_0 \end{aligned} \tag{23}$$

It is worth to remind that representations (19) and (23) are valid when the distance between the two groups $\vec{\mathbf{R}} = \vec{\mathbf{r}}_{ab}$ is greater than the distance $\vec{\mathbf{d}} = \left|\vec{\mathbf{r}}_{ma} - \vec{\mathbf{r}}_{nb}\right|$. For the cells belonging to groups not satisfying that condition, matrix entries L_{mn} and P_{mn} must be evaluated by the rigorous formulas (16) and (20).

4.3 Elementwise expansion of FMM-PEEC parameters

The matrix interpretation of FMM-based computation of PEEC parameters can be found. The matrix interpretation of one-dimensional FMM of complexity $O(n \log n)$ is well presented in [19]. A matrix version of FMM for the Laplace equation can be found in [20]. It is useful to give the same perspective also in the computation of PEEC parameters. The matrix version is more than a mere replacement for multiple summations and recursions by a clean matrix notation. The matrix viewpoint may help make the FMM more understandable to scientists and engineers who may want to use FMM for their computations.

The basic idea of the FMM is to establish a matrix factorization from an analytic elementwise expansion. This means that the FMM allows representing the Green's function in terms of matrix products.

Let us consider two basis functions whose centers $\vec{\mathbf{r}}_m$ and $\vec{\mathbf{r}}_n$ are well separated in the sense that conditions for applying the Gegenbauer's addition theorem are satisfied. As stated above the integration on the unit sphere is performed by using Gauss-Legendre integration with L+1 points for the integral over θ and uniform integration with 2(L+1) points for the integral over ϕ. Let us assume as auxiliary variable $u = \cos\theta = \hat{\mathbf{k}}_0 \cdot \hat{\mathbf{R}} \in [-1,1]$, let w_u and w_ϕ be the row vectors of the quadrature weights, Δu and $\Delta\phi$ the angular step for the integration over u and ϕ respectively. Furthermore, for a fixed order L of the multipole expansion, functions $F_m^v(\hat{\mathbf{k}}_0)$, $S_n^v(\hat{\mathbf{k}}_0)$, $F_m^S(\hat{\mathbf{k}}_0)$ and $S_n^S(\hat{\mathbf{k}}_0)$ can be regarded as matrices of order (L+1)x(2L+2). For a pair of inductive or capacitive cells m and n belonging to two well separated groups a and b function α_{ab}^L is also represented by a matrix of order (L+1)x(2L+2) when the vector $\hat{\mathbf{k}}_0$ varies on the unit sphere. It is clearly seen that the computation of the mutual partial inductance $L_{p,mn}$ and potential coefficient P_{mn} by FMM can be re-cast in a matrix form as

$$L_{p,mn} = \cos\theta_{mn}\, w_\phi \Delta\phi (F_m^v \,\square\, \alpha_{ab}^L \,\square\, S_n^v) w_u^T \Delta u \tag{24a}$$

$$P_{mn} = w_\phi \Delta\phi (F_m^S \,\square\, \alpha_{ab}^L \,\square\, S_n^S) w_u^T \Delta u \tag{24b}$$

where $\square$ denotes the Hadamard (elementwise) product of two matrices.

5 Fast matrix-vector product

It is well known that solving matrix equations arising from integral methods such as PEEC becomes more and more time demanding with the increase of the number of unknowns. When the discretization of the integral equation results in a total number of unknowns larger than some thousands direct solvers are not useful and iterative methods must be used. Their computational cost is $O(N^2)$, N being the matrix order and it is equal to the cost of a single full matrix-vector multiplication. Obviously it is important to speed-up this product as much as possible. In applying the MNA it is required calculating many matrix-vector products, involving the partial inductances L_P and potential coefficients P matrices. Evaluating a matrix-vector multiplication is equal to compute the effect at a given observation point $\vec{\mathbf{r}}$ due to all the sources, currents and charges. For a single observation point the contribution from neighbor groups is evaluated by using the exact formula given by (16) and (20). The contribution from far groups is calculated using the FMM-based formulas (19) and (23). The two terms are finally added to obtain the total effect. In the following we will refer to the matrix-vector product $j\omega L_P I_L$ but the same considerations can be done for the PQ product.

The idea is to divide the current sources into G groups. Each of them contains approximately N/G cells. Let us denote G_a the set of cells which belong to group a. For each group of cells the near and far field region are found. Let N_a the set of groups which are near neighbors to group a.

$$N_a = \left\{ b \,:\, \left|\vec{r}_a - \vec{r}_b\right| \le R \right\} \qquad a = 1,\ldots,G \tag{25}$$

where R is the distance beyond which two groups are considered far neighbors.
In order to better explain how the method works let us consider the relation giving the magnetic vector potential at location $\vec{r}_m$ belonging to group G_a generated by the current flowing in the cell n belonging to group G_b.

$$\vec{\mathbf{A}}(\vec{r}_m,\vec{r}_n)=\frac{\mu}{4\pi}\int_{V_n}G(\vec{r}_m,\vec{r}_n)\vec{\mathbf{J}}(\vec{r}_n)\,dV_n \tag{26}$$

The total magnetic vector potential due to all the current sources can be calculated considering separately the contributions from the near neighbors groups and that from far groups. This can be done mathematically as

$$\begin{aligned}\vec{\mathbf{A}}(\vec{r}_m)=&\sum_{b\in N_a}\sum_{n\in G_b}\frac{\mu}{4\pi S_n}\int_{V_n}G(\vec{r}_m,\vec{r}_n)i_n\hat{\mathbf{u}}_n\,dV_n+\\&+\frac{\mu}{4\pi}\int_{k_0}e^{j\vec{\mathbf{k}}_0\bullet\vec{\mathbf{r}}_{ma}}\sum_{b\notin N_a}\alpha_{ab}^{L}\left(\hat{\mathbf{r}}_{ab}\bullet\hat{\mathbf{k}}_0\right)\left[\sum_{n\in G_b}\left(\frac{1}{S_n}\int_{V_n}e^{-j\vec{\mathbf{k}}_0\bullet\vec{\mathbf{r}}_{nb}}dV_n\right)i_n\hat{\mathbf{u}}_n\right]\qquad \text{for } m=1,\ldots,N\end{aligned} \tag{27}$$

where it has been assumed $\vec{\mathbf{J}}(\vec{r}_n)\cong\frac{i_n}{S_n}\hat{\mathbf{u}}_n$. It can be easily seen that the evaluation of the contribution of the far groups to the magnetic vector potential at point $\vec{r}_m$ is carried out in three steps. In the first one it is calculated the field at each group center due to the sources of the group.

$$\vec{\mathbf{A}}_1(\vec{r}_b,k_0)=\left[\sum_{n\in G_b}\left(\frac{1}{S_n}\int_{V_n}e^{-j\vec{\mathbf{k}}_0\bullet\vec{\mathbf{r}}_{nb}}dV_n\right)i_n\hat{\mathbf{u}}_n\right]\qquad \text{for } b=1,\ldots,G \tag{28}$$

In the second stage the field is translated from one group's center to another one. This is represented by the calculation of

$$\vec{\mathbf{A}}_2(\vec{r}_a,k_0)=\sum_{b\notin N_a}\alpha_{ab}^{L}\left(\hat{\mathbf{r}}_{ab}\bullet\hat{\mathbf{k}}_0\right)\vec{\mathbf{A}}_1(\vec{r}_b,k_0)\qquad \text{for } a=1,\ldots,G \tag{29}$$

In the last step the field at each group center is scattered to each cell inside the group as follows:

$$\vec{\mathbf{A}}_3(\vec{r}_m)=\frac{\mu}{4\pi}\int_{k_0}e^{j\vec{\mathbf{k}}_0\bullet\vec{\mathbf{r}}_{ma}}\vec{\mathbf{A}}_2(\vec{r}_a,k_0)d^2\hat{\mathbf{k}}_0\qquad \text{for } m=1,\ldots,N \tag{30}$$

The total magnetic vector potential at point $\vec{r}_m$ can be finally obtained as

$$\vec{\mathbf{A}}(\vec{r}_m) = \sum_{b\in N_a}\sum_{n\in G_b} \frac{\mu}{4\pi S_n}\int_{V_n} G(\vec{r}_m,\vec{r}_n)\, i_n \hat{\mathbf{u}}_n \, dV_n + \vec{\mathbf{A}}_{\mathbf{3}}(\vec{r}_m) \quad \text{for } m = 1,\ldots,N \tag{31}$$

In accordance to the standard PEEC method the inner product of a vector function $\vec{f}$ with the unit vector $\hat{\mathbf{u}}_m$ is defined as

$$\left\langle \vec{f} \,\middle|\, \hat{\mathbf{u}}_m \right\rangle = \frac{1}{S_m}\int_{V_m} \vec{f}(\vec{r}_m) \bullet \hat{\mathbf{u}}_m \, dV_m \tag{32}$$

The inner product of $\vec{\mathbf{A}}(\vec{r}_m)$ with $\hat{\mathbf{u}}_m$ yields

$$\begin{aligned} \left\langle \vec{\mathbf{A}}(\vec{r}_m) \middle| \hat{\mathbf{u}}_m \right\rangle &= \sum_{b\in N_a}\sum_{n\in G_b} \frac{\mu}{4\pi\, S_m S_n}\int_{V_m}\int_{V_n} G(\vec{r}_m,\vec{r}_n)\, i_n \hat{\mathbf{u}}_m \bullet \hat{\mathbf{u}}_n \, dV_m dV_n + \\ &+ \frac{1}{S_m}\int_{V_m} \hat{\mathbf{u}}_m \bullet \vec{\mathbf{A}}_{\mathbf{3}}(\vec{r}_m) dV_m \quad \text{for } m \in G_a,\ n \in G_b \end{aligned} \tag{33}$$

The induced voltage on the inductive cell *m* due to all the current basis functions is obtained as

$$\begin{aligned} \sum_n j\omega L_{p,mn} I_{L,n} = j\omega \sum_n \left\langle \vec{\mathbf{A}}(\vec{r}_m) \middle| \hat{\mathbf{u}}_m \right\rangle &= j\omega \sum_{b\in N_a}\sum_{n\in G_b} \frac{\mu}{S_m S_n}\int_{V_m}\int_{V_n} G(\vec{r}_m,\vec{r}_n)\, i_n \hat{\mathbf{u}}_m \bullet \hat{\mathbf{u}}_n \, dV_m dV_n + \\ &+ \frac{j\omega}{S_m}\int_{V_m} \hat{\mathbf{u}}_m \bullet \vec{\mathbf{A}}_{\mathbf{3}}(\vec{r}_m) dV_m \quad \text{for } m = 1,\ldots,N \end{aligned} \tag{34}$$

where $\hat{\mathbf{u}}_m \bullet \hat{\mathbf{u}}_n = \cos\theta_{mn}$ takes into account the angle between the direction of the current basis functions *m* and *n*. Equation (34) provides a multipole representation of the magnetic field coupling between currents. The first term in equation (34) represents the contribution from the near neighbors groups, including the self group and the self cell. The second term in equation (34) takes into account the contribution from non-near neighbors groups. The same procedure can be applied to compute the potentials to infinity induced by charges, expressed by the matrix vector product PQ.

6 Numerical results

The accuracy of the computation of magnetic and electric field coupling in the PEEC method depends on the precision achieved in approximating the scalar Green's function by using Equation (12). In [17] it is shown that, if the number of digits of accuracy in the truncated Green's function is d_0, the order of expansion is given by $L = k_0 d + 1.8 d_0^{2/3} (k_0 d)^{1/3}$.

As a first test the scalar Green's function has been computed using an expansion order L=7, $\vec{\mathbf{r}}_{ab} = \vec{\mathbf{R}} = R\,\hat{\mathbf{z}}$, $\vec{\mathbf{d}} = 0.4\lambda\,\hat{\mathbf{z}}$. Fig. 4 shows magnitude (4a) and phase (4b) of the Green's function

evaluated by the exact formula (3) and that by means of (12) as function of the electrical distance between groups R/λ. Fig. 5 shows the relative error for various numbers of L.

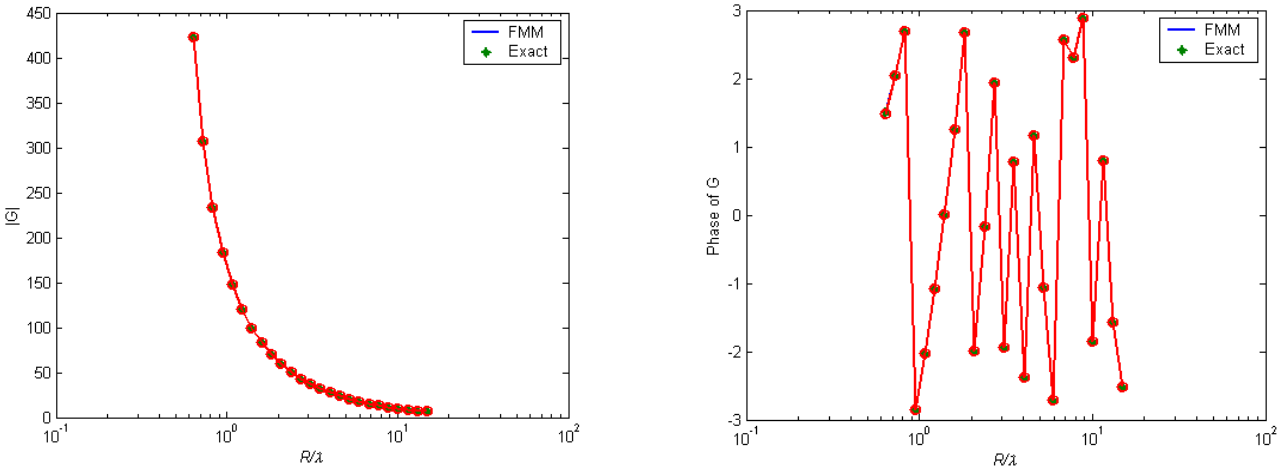

Fig. 4 – Green's function FMM approximation: (a) magnitude, (b) phase.

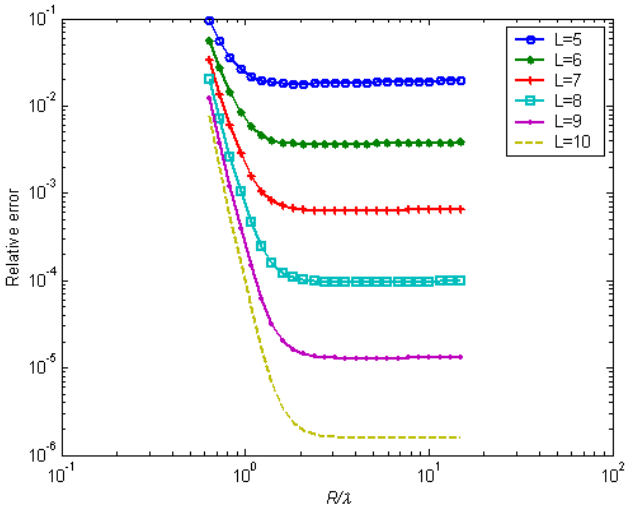

Fig. 5 – Relative error in the Addition Theorem for different number of terms.

As clearly seen the scalar Green's function is approximated accurately also for small electrical distances between groups ($R \approx \lambda$).

The second test has been done comparing partial inductances computed by means of Equation (16) and the FMM-based one (19) for various electrical distances between the corresponding groups. Two inductive cells m and n, of length $\lambda/10$ and cross section $\lambda/10 \times \lambda/100$ have been considered. By using the same notation as before, referring to the center of the basis functions domain, $\vec{\mathbf{r}}_m - \vec{\mathbf{r}}_n = \vec{\mathbf{R}} + \vec{\mathbf{d}}$ is assumed such that d is small enough to make R be close at $\left|\vec{\mathbf{r}}_m - \vec{\mathbf{r}}_n\right|$. Group center locations have been chosen such that d=0.4λ. Expansion order L=7 has been adopted. Fig. 6 shows

magnitude (6a) and phase (6b) of the mutual partial inductance $L_{p,mn}$ as function of the electrical distance between the groups.

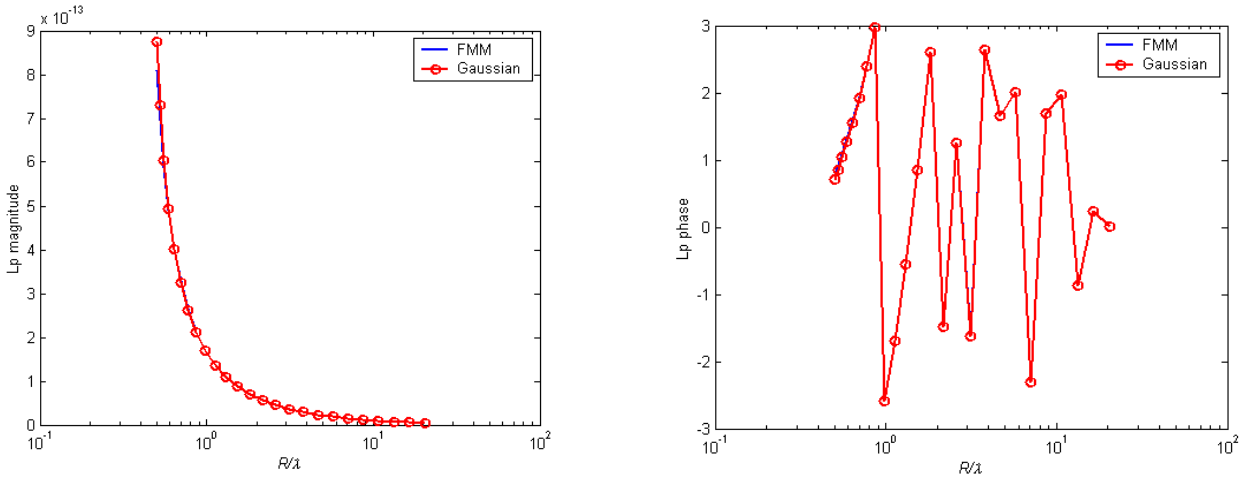

Fig. 6 – Partial inductances computation (L=7).

Further the relative error in the evaluation of $L_{p,mn}$ for different number of terms in the truncated series is shown in Fig. 7.

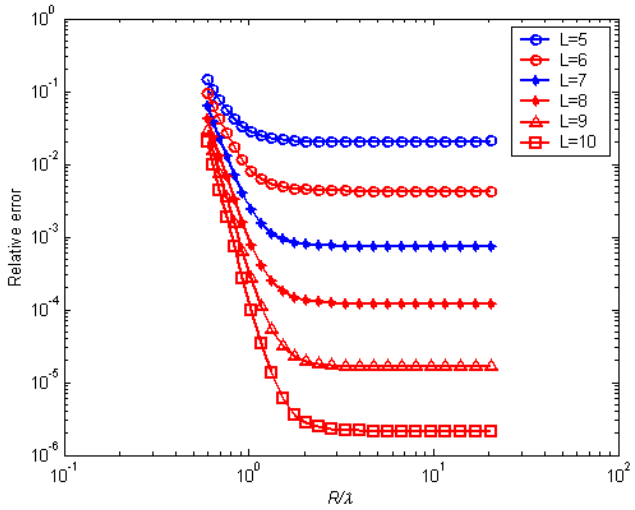

Fig. 7 – Relative error in the computation of partial inductances.

Even in this case a very good accuracy can be obtained also for electrically close groups. Further examples and tests cases can found in [18].

As final test partial inductances have been computed for different angular positions as shown in Fig. 8. Cells are $\lambda/10$ long and are characterized by a $\lambda/10 \times \lambda/100$ cross-section. Basis function have been chosen such that $|\vec{\mathbf{r}}_m - \vec{\mathbf{r}}_n| = 2\lambda$ and d=0.4 λ for all the different locations. Group centers are indicated by stars.

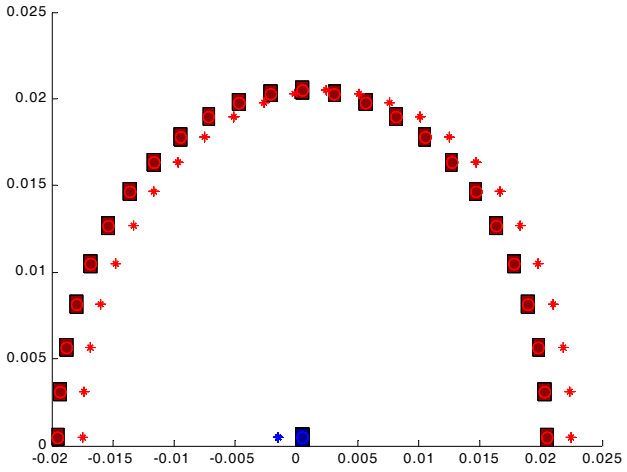

Fig. 8 – Basis function and group centers locations.

The corresponding values of magnitude and phase of partial inductances obtained by means of Gauss-Legendre integration and FMM are sketched in Fig. 9. The numerical integral (17) has been performed using an eight order Gauss-Legendre integration, FMM has been applied with L=10. As seen the accuracy is good for both magnitude and phase of $L_{p,mn}$.

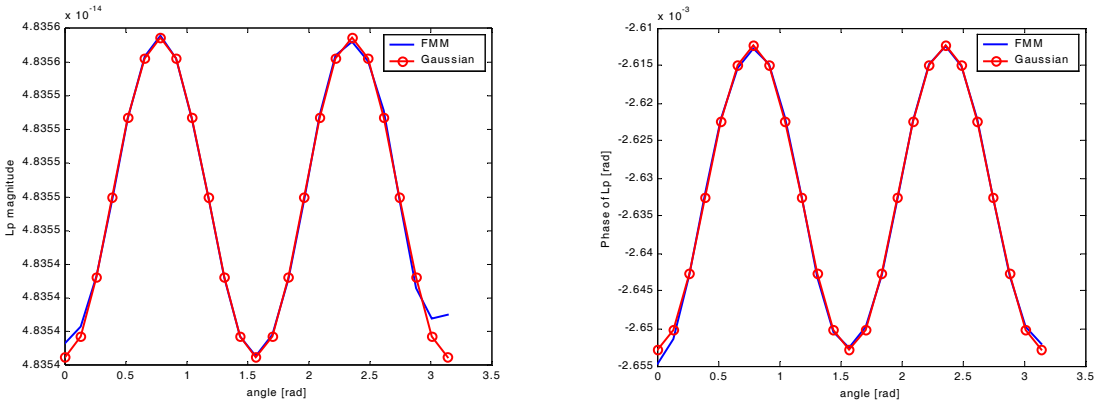

Fig. 9 – Partial inductance computation (L=10).

Finally the relative order in the computation of partial inductances $L_{p,mn}$ has been evaluated for different numbers of terms L in the range [5-10]. Two cell dimensions have been considered, $\lambda/4 \times \lambda/4$ and $\lambda/10 \times \lambda/10$ respectively, in order to investigate the impact of the cell dimension on the accuracy. The thickness is 0.01λ. The results are plotted in Fig. 10 confirming that acceptable 10^{-3} accuracy is obtained for orders L larger than 7 for both the dimensions.

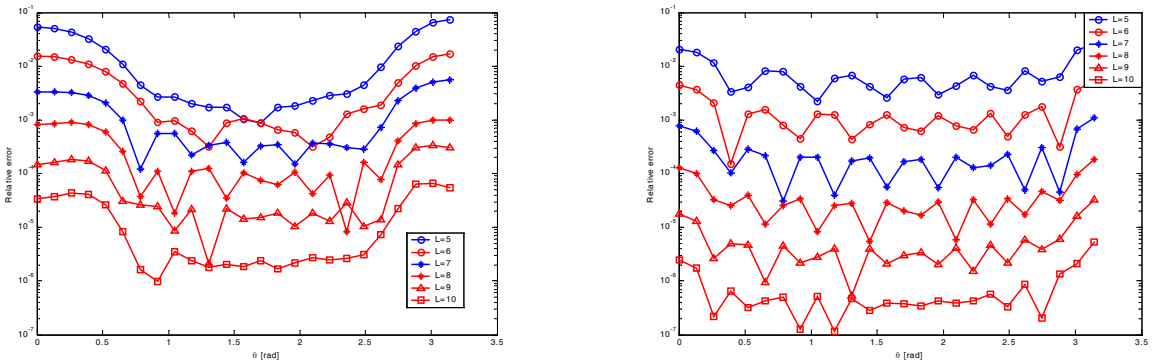

(a) (b)

Fig. 10 – Relative error for different expansion orders and cell dimension: (a) $\lambda/4$, (b) $\lambda/10$.

7 Conclusions

The paper has presented the application of the Fast Multipole Method to the Partial Element Equivalent Circuit Method. The use of the Addition Theorem allows to approximate the scalar Green's function in an accurate way introducing a de-coupling between non-near neighbor basis functions. A step-by-step implementation of coupling coefficients computation and matrix-vector product was then presented leading to multipole expressions for partial inductances and potential coefficients and a fast scheme to perform matrix-vector products as those arising from the MNA formulation. Several test have confirmed that good accuracy are achieved with relatively small orders of expansion.

References

[1] A.E. Ruehli, "Equivalent circuit models for three-dimensional multiconductor systems" *IEEE Trans. Microwave Theory Tech.*, vol. 22, n. 3, March 1974, pp 216-221.

[2] H.Heeb, A.E. Ruehli, "Three-Dimensional Interconnect Analysis Using Partial Element Equivalent Circuit" *IEEE Trans. on Circuits and Systems-1: Fundamental Theory and Applications*, vol.39, no. 11, November 1992, pp.974-981.

[3] A.E. Ruehli and H. Heeb, "Circuit Models for Three-Dimensional Geometries Including Dielectrics" *IEEE Trans. Microwave Theory Tech.*, vol. 40, n. 3, July 1992, pp. 1507-1516.

[4] Archambeault B., A. E. Ruehli, "Analysis of power/ground-plane EMI decoupling performance using the partial-element equivalent circuit technique", *IEEE Transactions on Electromagnetic Compatibility*, vol. 43, no.4, November 2001.

[5] C.C. Lu and W.C. Chew, "Fast algorithm for solving hybrid integral equations", *IEE Proceedings-H*, vol. 140, no. 6, pp.455-460, Dec. 1993.

[6] J.M. Song and W.C. Chew, "Multilevel fast-multipole algorithm for solving combined field integral equations of electromagnetic scattering", *Microwave Opt. Technol. Lett.*, vol.10, no.1, pp. 14-19, Sept. 1995.

[7] A.A. Ergin, B. Shanker, E. Michielssen, "The Plane-Wave Time-Domain Algorithm for the Fast Analysis of Transient Wave Phenomena", *IEEE Antennas Propagation Magazine*, vol. 41, no. 4, August 1999.

[8] B. Shanker, A.A. Ergin, E. Michielssen, “A Multilevel Plane Wave Time Domain Algorithm for the Fast Analysis of Transient Scattering Phenomena”, in *Proceedings of IEEE Antennas Propagat. Soc. Int. Symp.*, vol. 2, pp.1342-1345, Orlando, FL, July 11-16,1999.
[9] B. Shanker, A.A. Ergin, K. Aygün, E. Michielssen, "Analysis of Transient Electromagnetic Scattering Phenomena Using a Two-Level Plane Wave Time Domain Algorithm", *IEEE Transactions on Antennas and Propagation*, vol. 48, no. 4, April 2000, pp. 510 – 523.
[10] B. Shanker, A.A. Ergin, K. Aygün, E. Michielssen, “Analysis of Transient Electromagnetic Scattering from Closed Surfaces using a Combined Field Integral Equation”, *IEEE Transactions on Antennas and Propagation*, vol. 48, no. 7, July 2000.
[11] K. Aygun, B. Shanker, A.A. Ergin, E. Michiellsen, "A Two Level Plane Wave Time Domain Algorithm for Fast Analysis of EMC/EMI Problems" *IEEE Transactions on Electromagnetic Compatibility*, vol. 44, no.1, February 2002.
[12] C. Ho, A. Ruehli, P. Brennan, “The Modified Nodal Approach to Network Analysis”, IEEE Transactions on Circits and Systems, vol. CAS-22, pp. 504-509, June 1975.
[13] V. Rokhlin, "Rapid solution of integral equations of scattering theory in two dimensions", *J. Comput. Phys.*, vol. 86, no.2, pp. 414-439, Feb. 1990.
[14] R. Coifman, V. Rohklin, S. Wandzura, "The Fast Multipole Method for the Wave Equation: a Pedestrian Description", *IEEE Trans. Antennas Propagat.*, vol. 35, no. 3, pp.7-12, June 1993.
[15] M. Abramowitz and I.A. Stegun, *Handbook of Mathematical Functions*, New York: Dover Publications, 1972.
[16] G. Arfken, *Mathematical Methods for Physicists*, New York, NY, Academic Press, second edition, 1970.
[17] W.C. Chew, J.-M. Jin, E. Michiellsen, J. Song, *Fast and Efficient Algorithms in Computational Electromagnetic*, Artech House, 2001.
[18] G. Antonini, “The Fast Multipole Method for PEEC Circuits Analysis” in *Proc. of 2002 IEEE International Symposium on EMC*, Minneapolis, USA, August 2002.
[19] L. Greengard, V. Rokhlin, “A Fast Algorithm for Particle Simulations”, *Journal of Computational Physics*, (135):pp. 280-292, 1997.
[20] X. Sun, N. P. Pitsianis, “A Matrix Version of the Fast Multipole Method”, *SIAM Review*, 43(2):pp. 289-299, September 2001.